Journal of Engineering and Sustainable Development
Vol. 29, No. 06, November 2025
https://jeasd.uomustansiriyah.edu.iq/index.php/jeasd
ISSN 2520-0917
Research Article
https://doi.org/10.31272/jeasd.2493

Design Of Robotic Leg Using Proportional Integral Deferential Controller with Computed Torque Control Method

Zaineb Wared Matteb[1*], Sadeq Hussein Bakhy[2], Nabil Hassan Hadi[3]

[1,2]Mechanical Engineering Department, College of Engineering, University of Technology, Baghdad, Iraq
[3]Aeronautical Engineering Department, College of Engineering, University of Baghdad, Baghdad, Iraq.

[*]Email: eng.zaineb@uomustansiriyah.edu.iq

Article Info

Received 11/03/2024
Revised 18/04/2025
Accepted 01/05/2025

Abstract

Mobile robots are now crucial elements in manufacturing sectors. A five-link robot leg is fundamental for understanding the principles of robotic legs and is modelled by a nonlinear differential equation. Numerical solutions are used when closed-form solutions become difficult for systems with higher degrees of freedom. This study focused on controlling the robot leg to reach the desired position by combining computed torque control with a PID (Proportional Integral Derivative) controller derived from the motion equation. The numerical solution implemented in MATLAB includes simulation and modelling, with Simulink tools used to simulate dynamic systems, which are then evaluated against the computed torque control approach. Position errors for motor 1 and motor four were observed for 1 second and 10 seconds. Stability was achieved in the first motor after approximately 0.75 seconds. The second motor's movement stabilized after about 0.9 seconds, with the error between input and output for 10 seconds starting at 0.06 and 6.1, respectively, and stabilizing at zero within 1 second at motors 1 and 4, respectively. The system reached stability after approximately 0.3 seconds using computed torque with PID control, with gains (Kp, Kd, and Ki) set to (9500:10:20). Numerical simulation outcomes validate the controller's effectiveness in accurately tracking diverse trajectories.

Keywords: Computed torque control, Dynamic control, Five-bar mechanism, Mobile legged robot.

1. Introduction

Robot manipulators are widely acknowledged as complex, dynamically interconnected, and time-varying systems, extensively applied across various industries. These manipulators typically encounter uncertainties [1]. Due to robot manipulators' importance in all practical aspects, many researchers have addressed studying their control. During the studies, various control methods were employed, and there is a specific design aimed at improving the trajectory planning for the robot. As mentioned in [2], numerous studies on it make it possible to benefit from them in the design of control systems. Due to the difficulty of precisely controlling a robot manipulator to an accurate position, this task is challenging. For optimal performance, robots need to follow predefined trajectories closely. This emphasizes the significance of trajectory tracking control in the overall control of robotic manipulators [3]. Researchers introduced a strong control system for a six-degrees-of-freedom Stewart platform. The Newton-Euler method, combined with simplifying assumptions, is used to model the platform's dynamics precisely. The primary emphasis is on tracking the trajectory of ankle rehabilitation. The study uses the Computed Torque Control Law (CTCL) and Polynomial Chaos Expansion (PCE) to address uncertainties in geometric and physical parameters [4]. The proposed approach effectively manages uncertainties and eliminates system nonlinearity by integrating PCE with CTCL through feedback linearization. The analysis accounts for uncertainties in the patient's foot and moment-of-inertia parameters, using distributions such as uniform, beta, and normal [5], [6]. The investigation also encompasses PD control, PI control, feed-forward compensation control, adaptive control, variable structure control, and computed torque control [7], [8].

Some research explored the application of robust control to a 5-link bipedal robotic model using sliding mode control; it comprised the torso and two links in each leg, connected by four rotating joints [9]. It explained how the two-legged dynamic model was developed and how the torque and sliding-mode control algorithms were derived. Simulation results, with different levels of uncertainty and parameters [10].

A control strategy is proposed for the leg of a quadrupedal robotic system that utilizes electric quasi-direct-drive (QDD) actuators. To control the movement of the foot's tip, the control system implements a cascaded PID trajectory-tracking controller. The controller is responsible for regulating the angular velocity and position of every leg joint, allowing the robot to adhere to a predetermined trajectory while preserving maximum torque density and efficiency. By applying forward and inverse kinematics, both the intended path and the corresponding velocity of the foot's tip can be determined. The cascaded PID (Proportional Integral Derivative) controller functions as a low-level controller, guaranteeing accurate regulation of the robot's motion [11]. The assessment of the tracking and response performance of the robot manipulator across two input trajectories demonstrates that PID-CTC produces excellent accuracy and minimal error, thus solidifying its status as an effective motion control technique [12]. Adnan and Karam [13] developed the optimal Improved Proportional-Integral-Derivative (IPID) controller for a single-link human leg robot to track the intended path more effectively. However, the dynamic interaction and nonlinear coupling in multi-link robotic legs have not been adequately addressed. Most existing works either focus on simplified single-link or two-link manipulators or rely solely on conventional PID or CTC approaches, which often suffer from poor disturbance rejection, longer settling times, and trajectory tracking errors in multi-degree-of-freedom systems.

The main aim of this study is to design, model, and simulate a five-link robotic leg system that achieves precise trajectory tracking and fast stabilization by integrating a Proportional–Integral–Derivative (PID) controller with the Computed Torque Control (CTC) method. This integration is the novelty of this research, enhancing stability, accuracy, and convergence speed by combining model-based dynamic compensation in CTC with PID corrective feedback. The objective is to evaluate the performance of the hybrid CTC–PID controller in reducing position and velocity errors, enhancing dynamic stability, and ensuring accurate motion control of the robotic leg under nonlinear dynamic conditions.

2. Method of the Research

2.1 Dynamics of a Five-Link Mechanism

Numerical analysis of robotic legs involves the use of mathematical models and computational techniques to solve problems related to robot design and control. In this study, some key elements will be addressed, including:

- Forward Kinematics: Calculating the position and orientation of the robot's end-effector based on the joint values.
- Use of Numerical Algorithms: Used to solve complex differential and algebraic equations that describe the robot's motion.
- Development of Control Algorithms: Develop algorithms to control the robot's trajectory and ensure stability.

For analytical purposes, we employed a 2-DOF planar robot leg consisting of a five-bar mechanism, driven by two servo motors at points 1 and 4, and designed in SolidWorks, as depicted in Fig. 1(a).

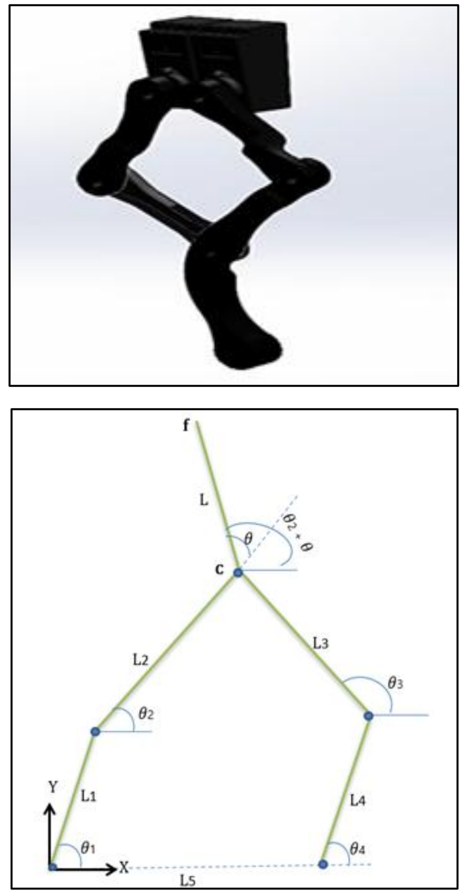

Figure 1. (a) The SolidWorks program designs the leg of the robot, and (b) Schematic of the 5-bar linkage robotic leg.

The forward kinematics equations for a 2-degree-of-freedom robotic manipulator have been derived and are presented in references [9] and [14]. The equations describe the foot tip's position in terms of the angles of the two joints. The foot tip's position is determined by combining the vectors from motor 1 to the foot link at point c. [9], [15], [16]:

$$\begin{aligned} xc &= L_1 * \cos\theta_1 + L_2 * \cos\theta_2 \\ yc &= L_1 * \sin\theta_1 + L_2 * \sin\theta_2 \end{aligned} \quad (1)$$

The foot tip position equations of adding up the vectors from motor 4 to the foot tip, going through $L_3, L4, and\ L_5$, in x and y directions:

$$\begin{aligned} xc &= L_3 * \cos\theta_3 + L_4 * \cos\theta_4 + L_5 \\ yc &= L_3 * \sin\theta_3 + L_4 * \sin\theta_4 \end{aligned} \quad (2)$$

Then, the position of point f the end of the foot with the ground:

$$xf = l_1 * \cos\theta_1 + l_2 * \cos\theta_2 + l * \cos(\theta + 2\arctan(\theta_2)) \quad (3)$$

$$yf = l_1 * \sin\theta_1 + l_2 * \sin\theta_2 + l * \sin(\theta + 2\arctan(\theta_2)) \quad (4)$$

To simplify matters, we assume that the center of mass of each link is located precisely at its midpoint. Additionally, we believe the gravitational force acts in the negative Y direction. Let's define $\theta = (\theta, \theta 4)^{T}$ as the generalized coordinates and denote T as the kinetic energy, U as the potential energy, and L' as the Lagrangian function, where $L' = k$ minus U. The kinetic energies of the system can be expressed as follows by utilizing the previously mentioned notations and considering the assumptions [17], [18]. Fig. 2 shows the kinematic computation flowchart.

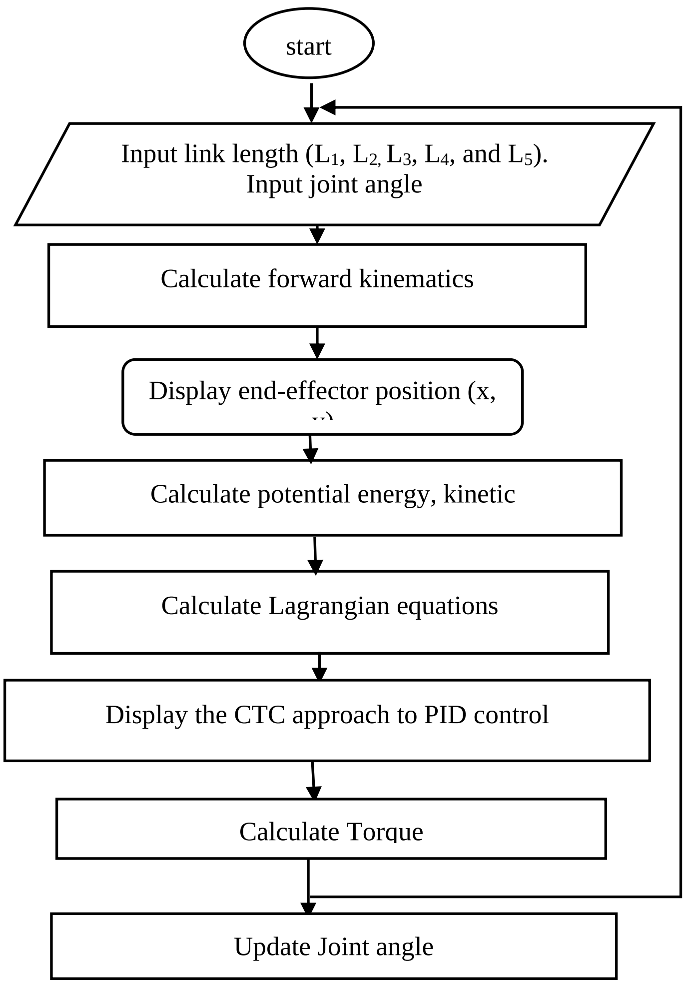

Figure 2. Flowchart for kinematic computation.

$$\begin{aligned} K = \ & \tfrac{1}{2}[(I_1 + m_1 L_{c1}^2 + m_2 L_1^2)\dot{q}_1^2 + (I_4 \\ & + m_4 L_{c4}^2 + m_3 L_4^2)\dot{q}_4^2 + 2m_2 L_4 L_{c3} \\ & C_{1-2}\dot{q}_1\dot{q}_2 + (I_3 + m_3 L_{c3}^2)\dot{q}_3^2 + 2m3 \\ & L_4 L_{c3} C_{3-4}\dot{q}_4\dot{q}_3 + (I_2 + m_2 L_{c2}^2)\dot{q}_2^2] \end{aligned} \quad (5)$$

Lagrangian equations:

$$\begin{aligned} L' = \ & \tfrac{1}{2}[(I_1 + m_1 L_{c1}^2 + m_2 L_1^2)\dot{q}_1^2 + (I_4 + m_4 \\ & L_{c4}^2 + m_3 L_4^2)\dot{q}_4^2 + 2m_2 L_4 L_{c3} C_{1-2}\dot{q}_1\dot{q}_2 \\ & + (I_3 + m_3 L_{c3}^2)\dot{q}_3^2 + 2m_3 L_4 L_{c3} C_{3-4}\dot{q}_4\dot{q}_3] \\ & + (I_2 + m_2 L_{c2}^2 \dot{q}_2^2) - m_1 g(L_{c1} S_1) - m_2 g \\ & (L_{c2} S_2 + L_1 S_1) - m_3 g(L_{c3} S_3 + L_4 S_4) - \\ & m_4 g(L_{c4} S_4) \end{aligned} \quad (6)$$

Then $\partial/\partial t$:

$$\frac{\partial}{\partial t}\left[\frac{\partial L}{\partial \dot{\theta}_i}\right] - \frac{\partial L}{\partial \theta_i} = T_i \ \text{where } i = 1, 2 \quad (7)$$

$$M(q)\dot{q}_i - C(q, \dot{q})\dot{q}_i + G(q) = \tau_i \quad (8)$$

$M(q)$ is the $n \times n$ inertia torques matrix of the 2-DOF LR system. $C(q, \dot{q})$ is an $n \times n$ matrix of the centrifugal and Coriolis torques of the 2-DOF LR. $G(q)$ is the $n \times 1$ gravitational torque vector. The parameters above, $M(q)$, $C(q, \dot{q})$ q, and $G(q)$, were calculated using MATLAB software for subsequent use in the simulation process of the system.

The numerical solution implemented using MATLAB encompasses diverse facets of simulation, specifically the construction of a dynamic system model for a robotic leg. The system dynamics were formulated through (8) and subsequently visualized using Simulink blocks. The simulation setup involved configuring parameters such as time steps, solver options, and initializing conditions, including defining a specific trajectory and input signals. The simulation was run to analyze the system's behavior comprehensively. Subsequently, a simulation analysis was conducted to assess the control system's performance. This was followed by an iterative process of adjusting gains through empirical testing informed by simulation results, aimed at mitigating errors and enhancing system control.

2.2. Design for PID Computed Torque Control of Robot Leg:

The equation of motion of the mechanical system with five linkages is simulated as shown in Fig. 3. Applying a servo control law to the equation of motion above yields a computed torque control system. Subsequently, any classical control law, such as PD, PI, or PID, can be employed.

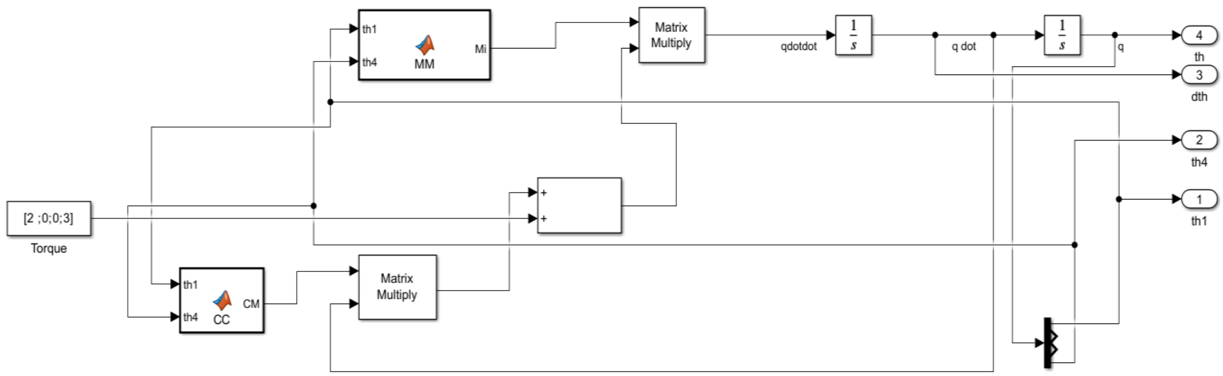

Figure 3. Five-bar leg robot simulation with MATLAB program.

The Computed Torque Control (CTC) method for robot control is a computationally intricate model-based approach. It relies on the system's dynamics model to calculate control signals, which are then input into the system. Unlike PID controllers, it addresses the challenges encountered in conventional control methods. The problems a Closed-Loop Transfer Control (CTC) system may encounter, which motivate the use of a PID controller, include oscillations, instability, increased deviation, and slow response time.

These problems arise from variations in system parameters, external disturbances, and changes in operating conditions. Here, a PID controller is used to effectively control the system's response, reducing oscillations and shortening the time to stability. Its operation is grounded in the system dynamics model, generating control signals to compensate for the rigid-body dynamics of the physical system. Particularly effective at higher speeds and accelerations, especially with substantial payloads, the CTC controller proves resilient to external disturbances such as changes in payload, as long as the payload dynamics are less significant than the system's dynamics under control [19]. In this case, a PID controller is used to improve the system's accuracy. Feedback control is implemented to achieve this. The combination of computed torque control and PID feedback control is referred to as the PID computed torque control method, a term commonly used in most studies employing this method, as in [20].

The complete system simulation, comparing the computed torque controller with PID, is illustrated in Fig. 4. The computed joint torque, which is the robot arm input, is given by:

$$\tau = M(\theta)\left(\dot{\theta}_d + K_d\dot{e} + K_p e + Ki\int e(t)dt\right) + C\left(\theta,\dot{\theta}\right)\dot{\theta} \quad (9)$$

The equation for the entire system can be derived from (8) and (9) by:

$$M(\theta)\dot{\theta} + C\left(\theta,\dot{\theta}\right)\dot{\theta} = M(\theta)\left(\ddot{\theta}_d + K_d\dot{e} + K_p e + Ki\int e(t)dt\right) + C\left(\theta,\dot{\theta}\right)\dot{\theta} \quad (10)$$

Where $\dot{\theta} = \ddot{\theta}_d + K_d\,\dot{e} + K_p e + Ki\int e(t)dt$ (11) [21].

To improve tracking performance, the gain parameters K_d and K_p should be adjusted using standard control methods from linear control theory. The gain matrices K_d, Ki, and K_p can be diagonal matrices with positive entries. This makes the closed-loop system linear, decoupled, and exponentially stable. This way of controlling things has significant benefits. It refers to the procedure that modifies these variables to attain the system's intended performance. Conventional approaches, such as trial-and-error procedures, are applied. The goal of tuning is to get the system to respond as intended while preserving stability and lowering control error.

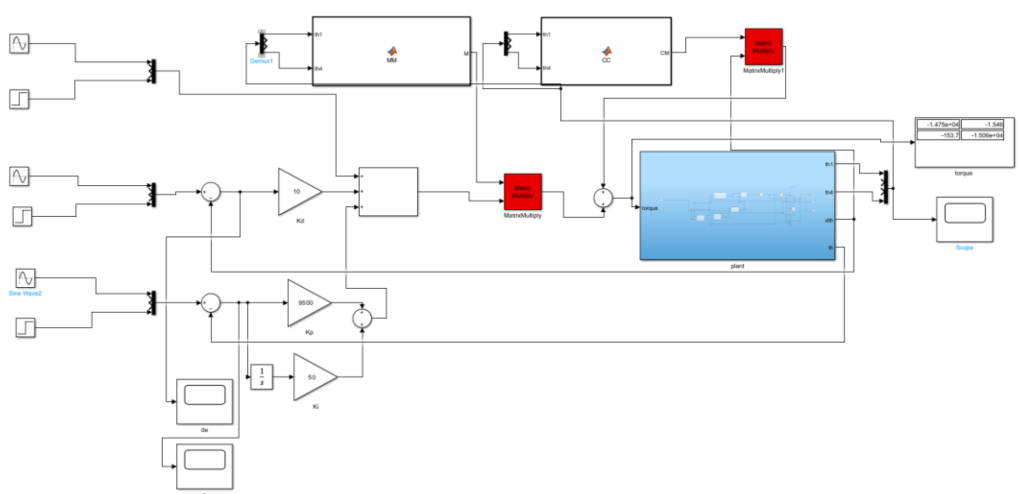

Figure 4. Computed torque controller with PID controller feedback loop for leg robot model.

3. Results of Simulation

For simulation purposes, the following values are taken in MATLAB programming: Total Simulation Time = T1 = 10 sec.

Gains:

$$K_p = [9500000; 0000; 0000; 0009500];$$

$$K_d = [10000; 0000; 0000; 00010];$$

$$Ki = [20000; 0000; 0000; 00020];$$

Simulation is conducted to validate the outcomes of the suggested control approach. The simulation is performed for 10 seconds. At intervals of 0.002 seconds, sample readings are taken to generate the plotted graphs. Fig. 5 shows position errors and velocity errors for motor 1 and motor before control. Fig. 6 illustrates the positional errors for motor 1 and motor 4 over 1 sec and at the initial. At the same time, Fig. 7 displays the velocity errors for motor one and motor two during the same time frame.

The simulation results depicted in Fig. 8 and Fig. 9 compare the actual and predicted positions of motor one and motor 4, respectively, over a period of 3 seconds. The percentage errors are approximately 0.052 and 0.0023 for motor one and motor 4, respectively. Fig. 10 illustrates the torque required for actuators 1 and 4 for the computed torque controller over a duration of 10 seconds. During the initial operation of the system, oscillations were observed, which eventually stabilized at around 1.2 seconds, indicating the optimal time to achieve a stable state.

An error in the trajectory planning was detected for one leg of the mobile robot, as the desired trajectory was compared with the one derived from (3) and (4). As illustrated in Fig. 11, the error at x initially reaches 0.02 and gradually decreases until it stabilizes around zero at approximately 3 seconds, and then remains stable. Regarding the y-direction trajectory error shown in Fig. 12, it initially oscillates, then reaches a steady state after 4 seconds, and remains stable thereafter. Readings were taken up to the trajectory error of 40 seconds.

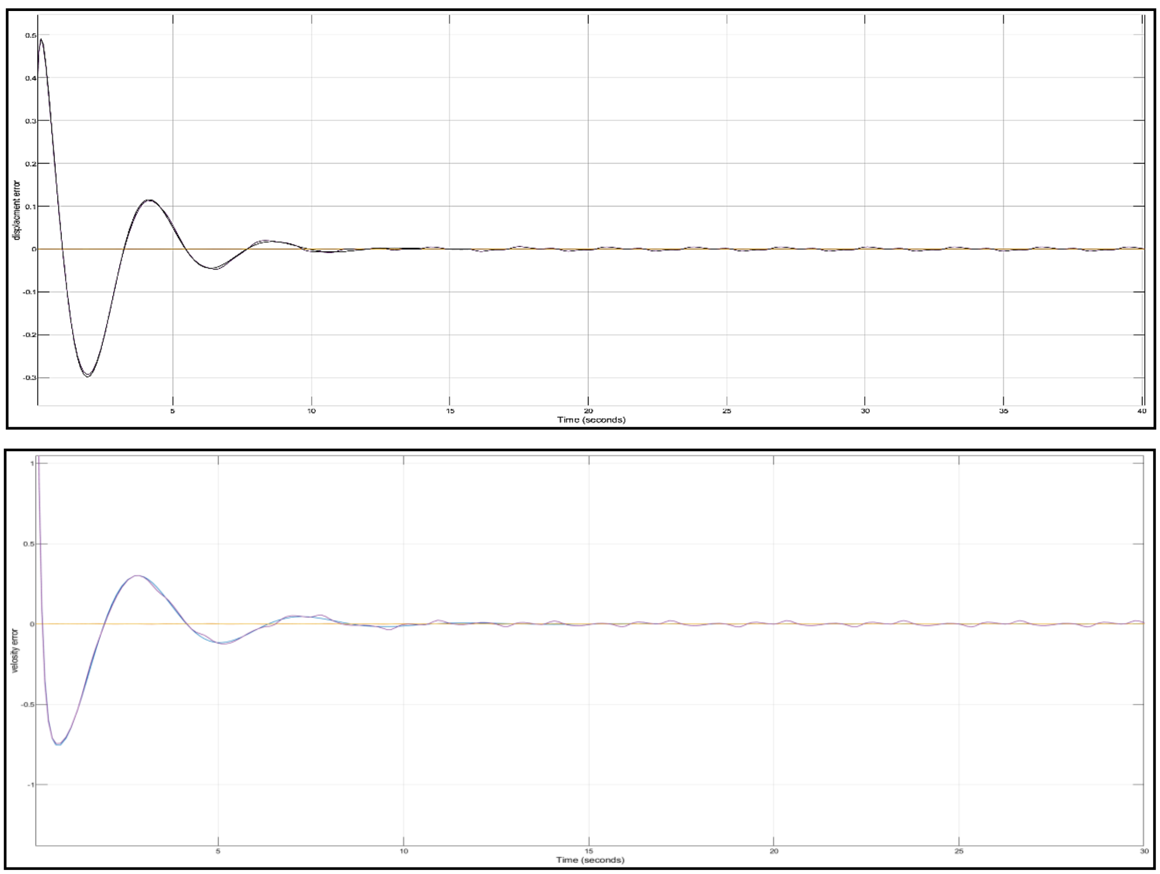

Figure 5. Position errors and Velocity errors for motor 1 and motor before control.

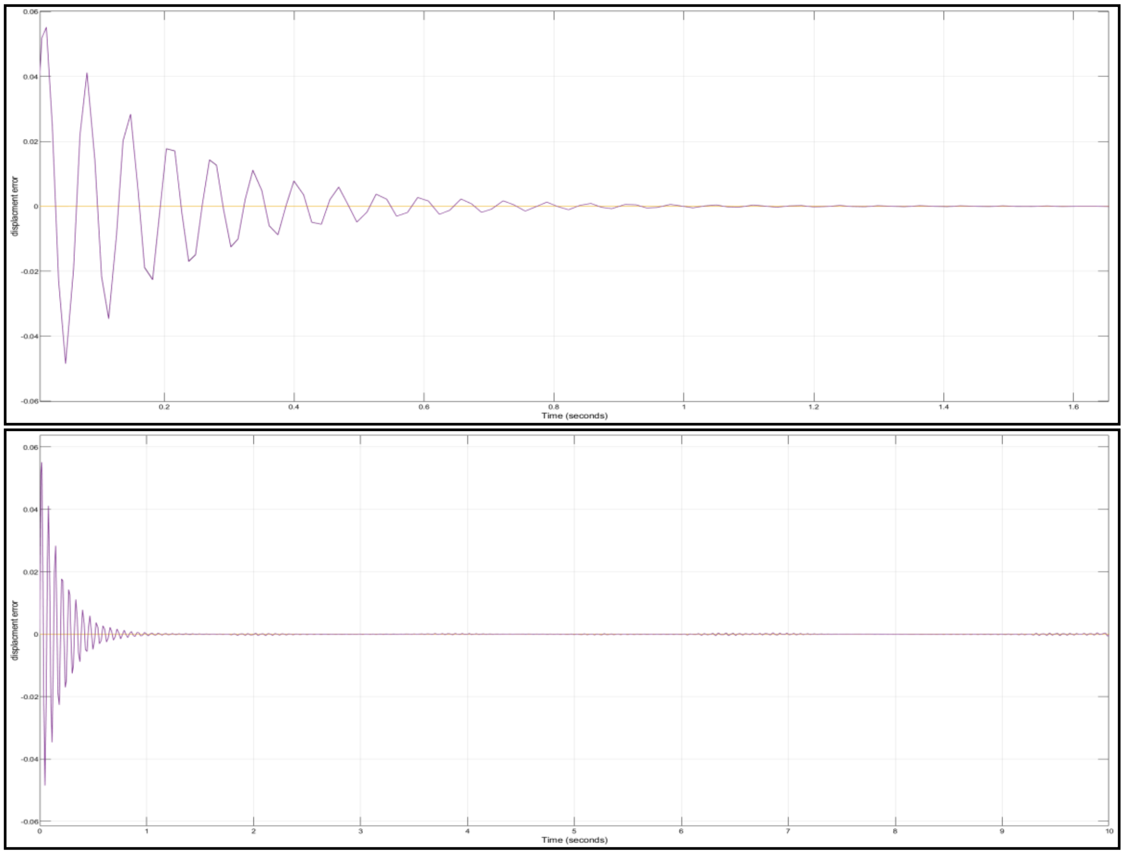

Figure 6. Position errors for motor 1 and motor 2 for 1 sec and 10 sec.

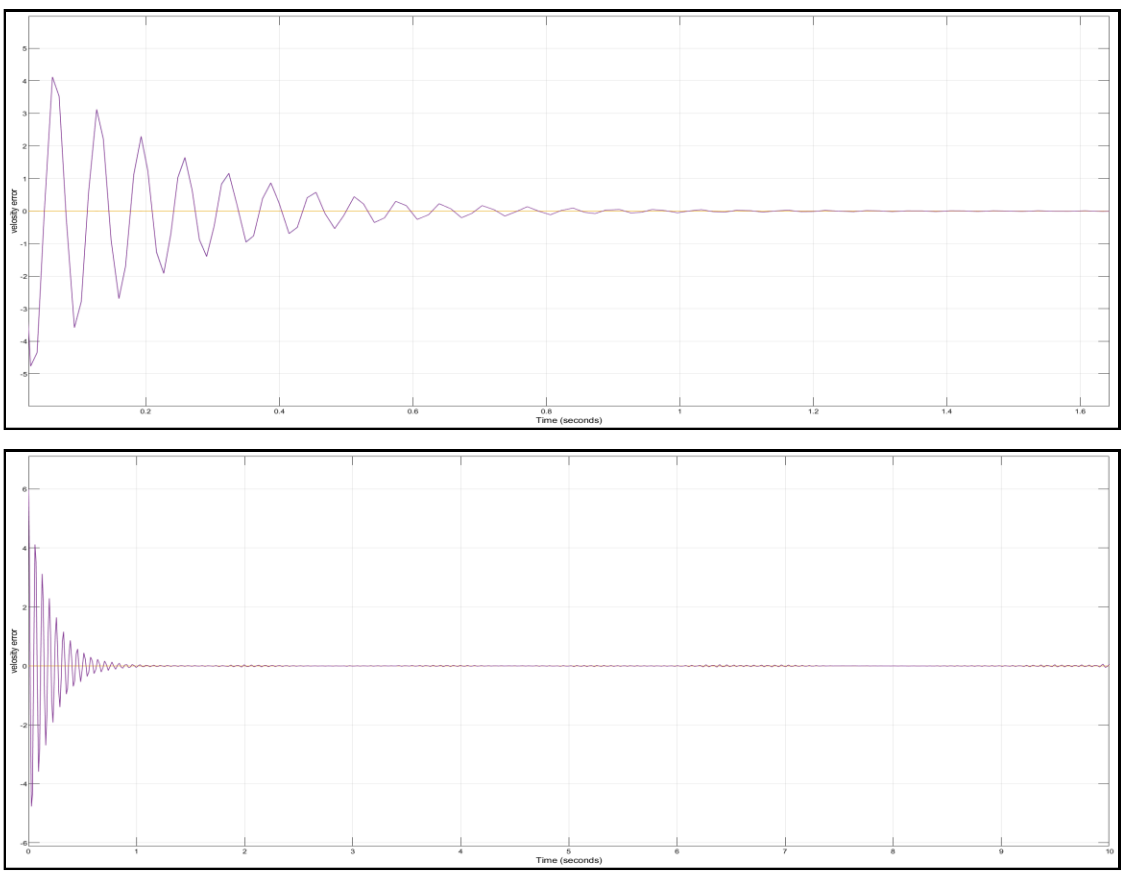

Figure 7. Velocity errors for motor 1 and motor 2 for 1 sec and 10 sec.

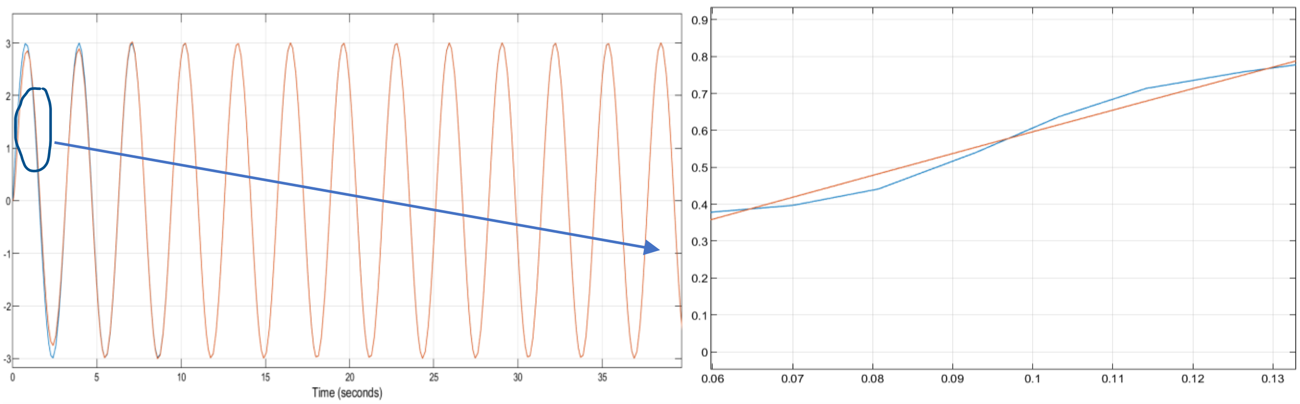

Figure 8. The comparison of the derived position for motor 1

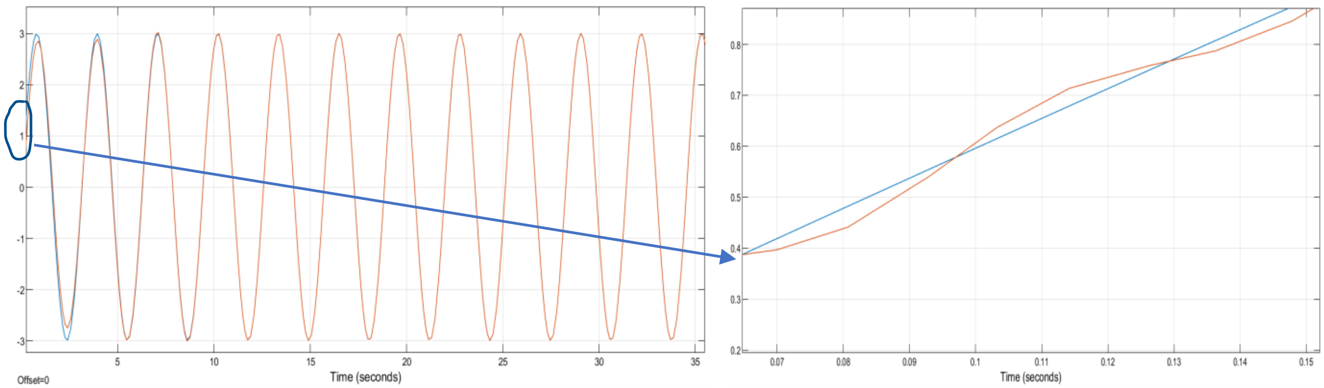

Figure 9. The comparison of the derived position for motor 4

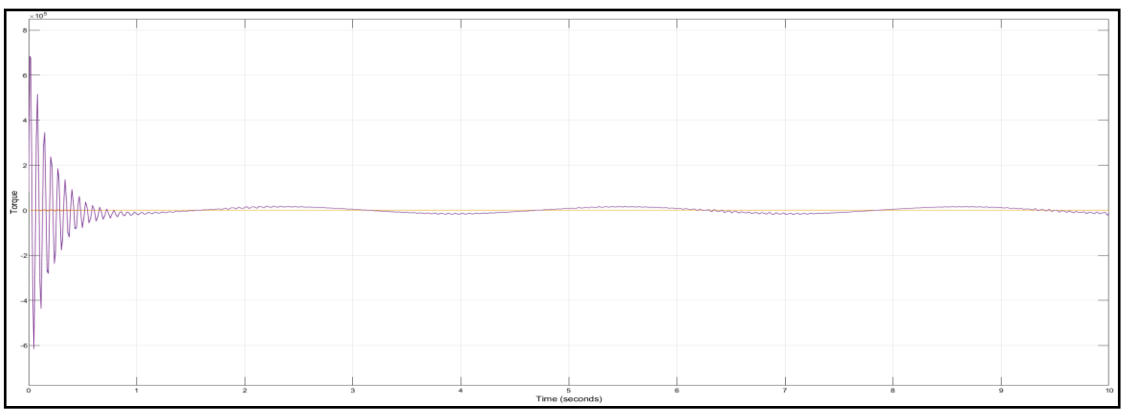

Figure 10. The torque required for the five-bar robot leg for 10 seconds.

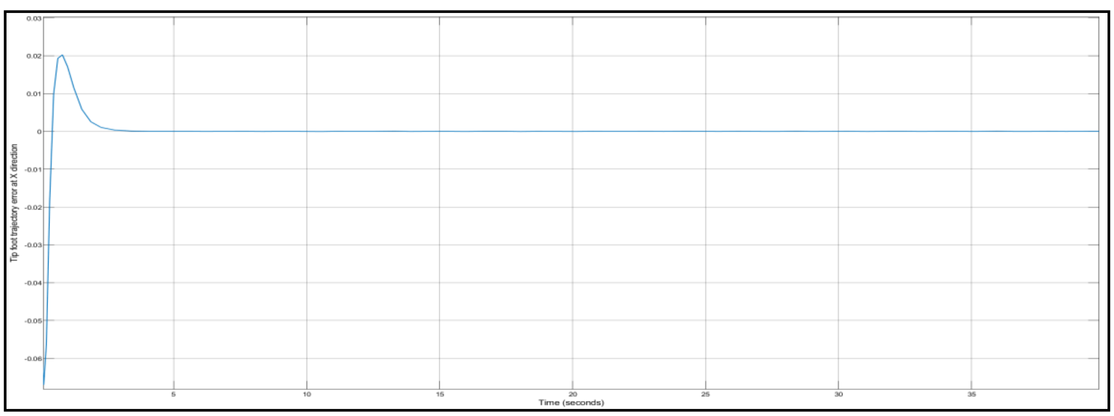

Figure 11. Trajectory error at x-distance at gait planning for the five-bar robot leg at the tip of the foot for 40 seconds.

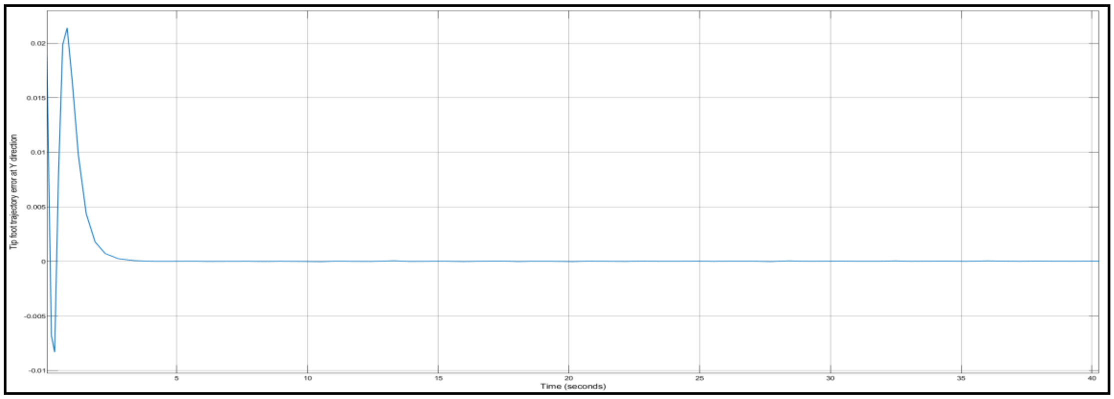

Figure 12. Trajectory error at y-distance at gait planning for the five-bar robot leg at the tip of the foot for 40 seconds.

In general, it highlights the research's strengths, including the kinematic forward equation for the 5-bar-to-tip foot of one leg. The five-bar mechanism is actuated by two actuators (passive and active joints), and the simulation of the nonlinear dynamic equations of the four legs is performed.

Numerical simulation results validate the effectiveness of the proposed controller in accurately tracking diverse trajectory types, as demonstrated by comparing it with previous studies [3], [15] which document the success of their approaches through simulation results using PID controllers, highlighting advancements in robotic control and design principles relevant to the field. Each study focuses on numerical solutions and simulations in MATLAB for robotic systems, using control techniques such as kinematic model-based control and computed torque control with PID controllers. Although they differ in their specific applications (mining robotics versus robotic legs in manufacturing), the effectiveness of the control strategies is evident in both cases.

5. Conclusion

This research demonstrates the effectiveness of integrating a PID controller with Computed Torque Control (CTC) to control the nonlinear dynamics of a five-link robotic leg. It significantly improves trajectory tracking and stability compared with traditional PID methods. Simulation results show that the position error remained below 1%, while the velocity error did not exceed 7%, confirming high tracking precision and a smooth motion response. The hybrid controller achieved system stability within approximately 0.8 seconds, compared with about 1.5 seconds for conventional PID control. These results indicate significant improvements in settling time and accuracy, demonstrating the proposed control strategy's ability to manage nonlinear dynamic interactions in multi-link mechanisms.

Author Contributions Statement

All authors conducted the work equally.

Acknowledgments

The authors would like to thank Mustansiriyah University (www.uomustansiriyah.edu.iq), Baghdad, Iraq, for its support in the current work. We would also like to acknowledge the support of the University of Technology.

Conflicts of Interest

The authors declare no conflict of interest.

Symbol and Abbreviations

Symbol	Description
θi	The joint angle of joint i
mi	The mass of link i
Li	The length of link i
g	Gravitational acceleration (9.81) m/s2
xf	The position of the end of the foot with the ground in the x direction
yf	The position of the end of the foot with the ground in the y direction
Ci	cos θi
Si	sin θi
Ii	Mass moment of inertia of link i
Lci	Center of mass for links
L'	Lagrangian function
T	Kinetic energy
U	Potential energy
Kd	Derivative gain
Ki	Integral gain
Kp	Proportional gain
M(q)	Inertia torques matrix of LR
τ	Torqu
DOF	Degree Of Freedom
PID	Proportional Integral Derivative
PD	Proportional Derivative
PI	Proportional Integral
CTC	Computed Torque Control
e	Error
GOA	Grasshopper Optimization Algorithm
PCE	Polynomial Chaos Expansion
$\dot{\theta}$	Velocity vector
$\ddot{\theta}$	Acceleration vector

Reference

[1] A. A. Khalate, Gopinathan Leena, and G. Ray, "An Adaptive Fuzzy Controller for Trajectory Tracking of Robot Manipulator," *Intelligent Control and Automation*, vol. 02, no. 04, pp. 364–370, Jan. 2011, doi: https://doi.org/10.4236/ica.2011.24041

[2] SK Mahmood, SH Bakhy, MA Tawfik. "Motion Analysis and Trajectory Tracking Control of Propeller-Type Climbing Robot". *2nd Annual International Conference on Information and Sciences (AiCIS)*, Fallujah, Iraq. Nov, 2020. https://doi.org/10.1109/AiCIS51645.2020.00016

[3] G. Nandy, B. Chatterjee, and A. Mukherjee, "Dynamic Analysis of Two-Link Robot Manipulator for Control Design," *Lecture Notes in Electrical Engineering*, pp. 767–775, 2018, doi: https://doi.org/10.1007/978-981-10-7901-6_83.

[4] E. Khanbabayi and M.-R. S. Noorani, "Design Computed Torque Control for Stewart Platform with Uncertainty to the Rehabilitation of Patients with Leg Disabilities," *Computer Methods In Biomechanics And Biomedical Engineering*, vol. 27, no. 8, pp. 1028–1041, Jun. 2024, doi: https://doi.org/10.1080/10255842.2023.2222863.

[5] P. Chotikunnan and R. Chotikunnan, "Dual Design PID Controller for Robotic Manipulator Application," *Journal of Robotics and Control (JRC)*, vol. 4, no. 1, pp. 23–34, Feb. 2023, doi: https://doi.org/10.18196/jrc.v4i1.16990

[6] K. Ba et al., "Dynamics Compensation of impedance-based Motion Control for LHDS of Legged Robot," *Robotics and Autonomous Systems*, vol. 139, pp. 103704–103704, Nov. 2020, doi: https://doi.org/10.1016/j.robot.2020.103704.

[7] T. Zhou et al., "Adaptive Control for Manipulators with Unknown Virtual Control Coefficients and Input Nonlinearities," *IET Control Theory and Applications*, vol. 16, no. 11, pp. 1063–1074, Apr. 2022, doi: https://doi.org/10.1049/cth2.12285

[8] L. Shi, H. Yao, M. Shan, Q. Gao, and X. Jin, "Robust Control of a Space Robot Based on an Optimized Adaptive Variable Structure Control Method," *Aerospace Science and Technology*, vol. 120, pp. 107267–107267, Dec. 2021, doi: https://doi.org/10.1016/j.ast.2021.107267.

[9] K. V. Sancak and Z. Y. Bayraktaroglu, "Nonlinear Computed Torque Control of 6-Dof Parallel Manipulators," *International Journal of Control Automation and Systems*, vol. 20, no. 7, pp. 2297–2311, Jun. 2022, doi: https://doi.org/10.1007/s12555-021-0198-6

[10] F. Sedghi, S Neisarian, M. M. Arefi, M. H. Asemani, and Navid Vafamand, "Practical finite-time Adaptive Sliding Mode Control for 5-link Biped Robot in the Presence of Uncertainty," *International Journal of Control*, vol. 96, no. 8, pp. 1989–2002, May 2022, doi: https://doi.org/10.1080/00207179.2022.2079564

[11] A. M. El-Dalatony, T. Attia, H. Ragheb, and A. M. Sharaf, "Cascaded PID Trajectory Tracking Control for Quadruped Robotic Leg," *International Journal of Mechanical Engineering and Robotics Research*, vol. 12, no. 1, pp. 40–47, Jan. 2023, doi: https://doi.org/10.18178/ijmerr.12.1.40-47

[12] C. Feng, Z. Chen, W. Jin, and W. Guo, "Motion Control and Simulation Analysis of a Manipulator Based on Computed Torque Control Method," *Lecture notes in computer science*, pp. 10–22, Jan. 2023, doi: https://doi.org/10.1007/978-981-99-6483-3_2.

[13] A. Adnan and E. H. Karam, "Optimal Improved PID Controller with Goa Algorithm for Single Link Human Leg Robot," *Journal of Engineering and Sustainable Development*, vol. 26, no. 2, pp. 103–110, Mar. 2022, doi: https://doi.org/10.31272/jeasd.26.2.10.

[14] M. Ahmadizadeh, A. M. Shafei, and M. Fooladi, "Dynamic Modeling of closed-chain Robotic Manipulators in the Presence of Frictional Dynamic forces: a Planar Case," *Mechanics Based Design of Structures and Machines*, vol. 51, no. 8, pp. 4347–4367, Aug. 2021, doi: https://doi.org/10.1080/15397734.2021.1966304

[15] Q. He, G. Zhao, X. Shui, and K. Xu, "Kinematic Analysis and Simulation Study of 5R Robotic Arm," *In Ninth International Symposium on Sensors, Mechatronics, and Automation System, China (ISSMAS 2023)*, pp. 222–222, Mar. 2024, doi: https://doi.org/10.1117/12.3015018

[16] A.-A. Ayazbay, G. Balabyev, S. Orazaliyeva, K. Gromaszek, and A. Zhauyt, "Trajectory Planning, Kinematics, and Experimental Validation of a 3D-Printed Delta Robot Manipulator," *International Journal of Mechanical Engineering and Robotics Research*, vol. 13, no. 1, pp. 113–125, 2024, doi: https://doi.org/10.18178/ijmerr.13.1.113-125

[17] C. E. Ponce and D. A. Ponce, "A Didactic Approach to Energy-Based Dynamic Modeling: Least Action, D'Alembert Principle and Euler-Lagrange Formalism," *Lecture notes in networks and systems*, pp. 91–102, Jan. 2024, doi: https://doi.org/10.1007/978-3-031-47269-5_11

[18] Y. Li, J. Gao, W. Chen, Y. Zhou, and Z. Yin, "Simulation and Trajectory Optimization of Articulated Robots via Spectral Variational Integrators," *Communications in Nonlinear Science and Numerical Simulation*, vol. 131, pp. 107877–107877, Feb. 2024, doi: https://doi.org/10.1016/j.cnsns.2024.107877

[19] P. K. Khosla and Takeo Kanade, "Real-time Implementation and Evaluation of the computed-torque Scheme," *IEEE Transactions on Robotics and Automation*, vol. 5, no. 2, pp. 245–253, Apr. 1989, doi: https://doi.org/10.1109/70.88047.

[20] H. Badkoobehhezaveh, R. Fotouhi, and Q. Zhang, "Particle Swarm Optimization / PID-Computed Torque Control for a Manipulator," Volume 7: 46th Mechanisms and Robotics Conference (MR), Aug. 2022, doi: https://doi.org/10.1115/detc2022-89769

[21] A. Ibrahim Majeed, "Mobile Robot Motion Control Based On Chaotic Trajectory Generation," *Journal of Engineering and Sustainable Development*, vol. 24, no. 4, pp. 48–55, Jul. 2020, doi: https://doi.org/10.31272/jeasd.24.4.6.